

# Domain structure of ferroelectric ceramics

Toshio Ogawa

*Department of Electronic Engineering, Shizuoka Institute of Science and Technology 2200-2, Toyosawa, Fukuroi 437-8555, Japan*

Received 30 July 1999; received in revised form 8 September 1999; accepted 4 October 1999

## Abstract

PZT ceramics were statically and dynamically evaluated to examine the relationship between domain structures and electrical properties. We investigated the domain structures of tetragonal, M.P.B. and rhombohedral PZT ceramics at various poling fields to measure the poling field dependence of the crystal orientations and electrical properties as a statical evaluation. Furthermore, responses to repeated voltage pulses applied to the ceramics were measured by a high voltage test system as a dynamical evaluation. Through these evaluations, we could clarify the domain behavior for the 90° (71° or 109°) domain rotation, switching and clamping of 180° domain, and transient phenomena on the domain orientation. © 2000 Elsevier Science Ltd and Techna S.r.l. All rights reserved.

**Keywords:** Domain structure; Ferroelectric ceramics

## 1. Introduction

Ferroelectric random access memory (FRAM) devices composed of PZT thin films are attracting considerable attention. The degradation of the films due to domain switching, especially ferroelastic domain switching through 90° rotation (tetragonal phase) or 71° and 109° rotations (rhombohedral phase), needs to be reduced for the application. The evaluation and control of domain structures were recognized to be significant for the processes employed to develop materials for FRAM devices [1–4].

Domain switching in PZT ceramics can be caused by either or both mechanical stress and an electric field because the ceramics possess ferroelastic and ferroelectric properties. There are 90° (71° or 109°) and 180° domains in PZT ceramics, among which ferroelastic domain switching only occurs through 90° (71° or 109°) rotation. 90° and 71° (109°) rotations can be detected by changes in the peak intensities of {002} and {222} in X-ray diffraction (XRD), respectively. 180° switching, however, is independent of these peak intensities [5,6]. To confirm that the {002} and {222} peak intensities depended only on the 90° and 71° (109°) rotations, the rotations were measured by varying the poling field. We investigated the poling field dependence of the planar coupling factor,

the dielectric constant and the frequency constant, each of which is affected by both the 90° (71° or 109°) and 180° domains. We called the evaluation on the poling field dependence of the properties a statical evaluation. In addition, a pulse response measurement of the PZT ceramics was done as a dynamical evaluation. Through these evaluations, we clarified the relation between the domain switching and the electrical properties.

## 2. Experimental

The ceramic compositions were 0.05Pb(Sn<sub>1/2</sub>Sb<sub>1/2</sub>)O<sub>3</sub>–yPbTiO<sub>3</sub>–zPbZrO<sub>3</sub>, with 0.4 wt% MnO<sub>2</sub> [7], where  $y=0.62$ ,  $z=0.33$  (tetragonal phase),  $y=0.47$ ,  $z=0.48$  (M.P.B. phase) and  $y=0.20$ ,  $z=0.75$  (rhombohedral phase), respectively. The powders were uniaxially pressed at 150 MPa, and fired at 1240°C for 2 h. The fired sample disks were 14 mm in diameter and 1 mm thick. Poling was conducted at 80°C for 30 min while varying the poling field ( $E$ ) from  $0 \rightarrow +4.5$  (+3.0)  $\rightarrow 0 \rightarrow -4.5$  (–3.0)  $\rightarrow 0$  to +3.0 kV/mm. The crystal orientations of the PZT ceramics were examined using XRD for various values of  $E$ . The XRD intensity is expressed as the proportion of relative intensity  $I_{002} = I(002)/\{I(002) + I(200)\}$ , tetragonal) and  $I_{222} = I(222)/\{I(222) + I(\bar{2}22) + I(2\bar{2}2) +$

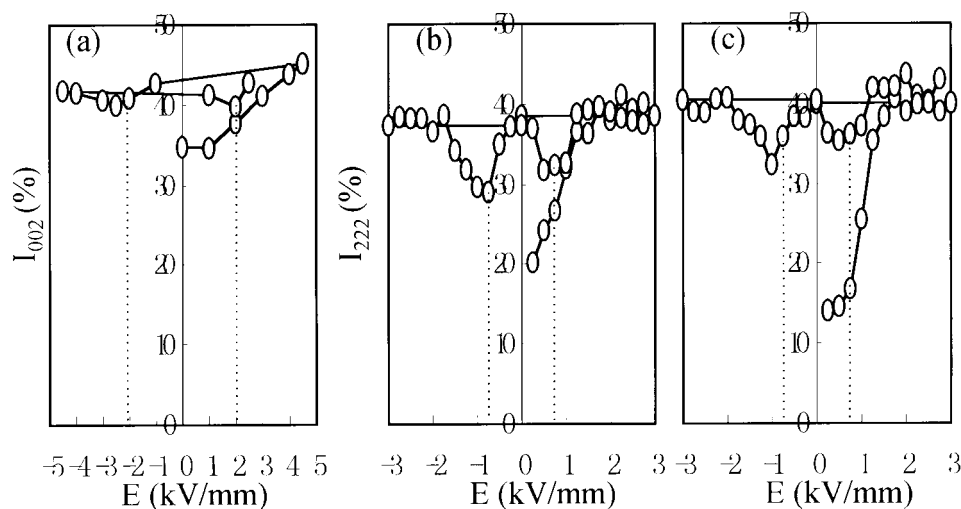


Fig. 1. Poling field ( $E$ ) dependence of XRD relative intensities ( $I_{002}$ ,  $I_{222}$ ) of: (a) tetragonal, (b) M.P.B. and (c) rhombohedral PZT ceramics.

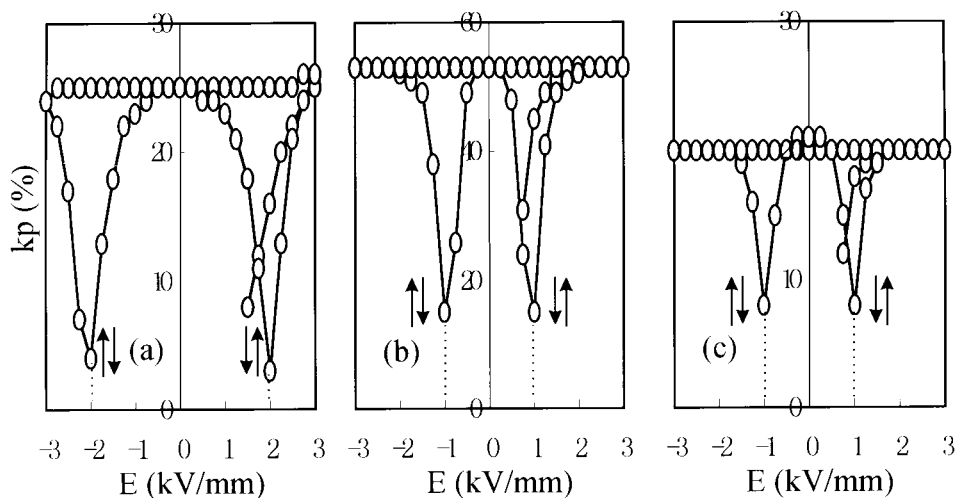


Fig. 2. Poling field ( $E$ ) dependence of planar coupling factor ( $k_p$ ) of: (a) tetragonal, (b) M.P.B. and (c) rhombohedral PZT ceramics.

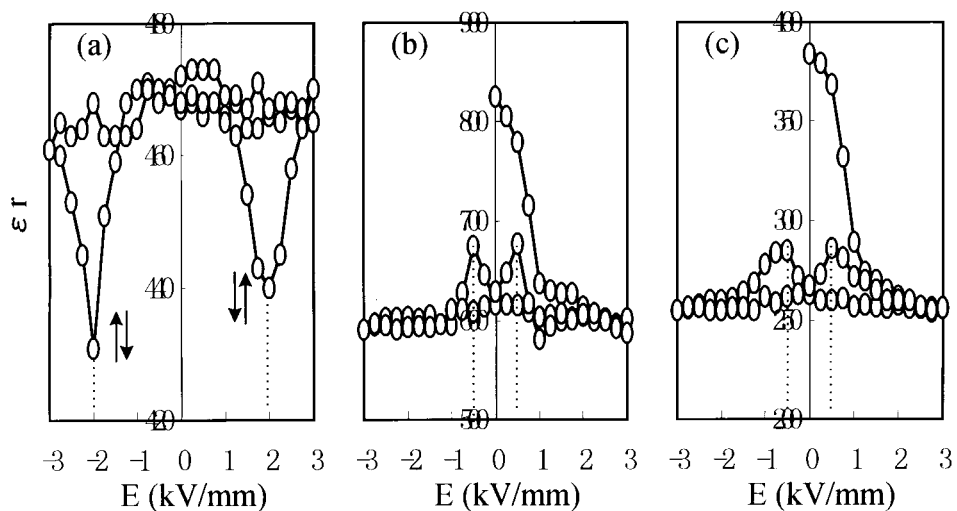


Fig. 3. Poling field ( $E$ ) dependence of dielectric constant ( $\epsilon_r$ ) of: (a) tetragonal, (b) M.P.B. and (c) rhombohedral PZT ceramics.

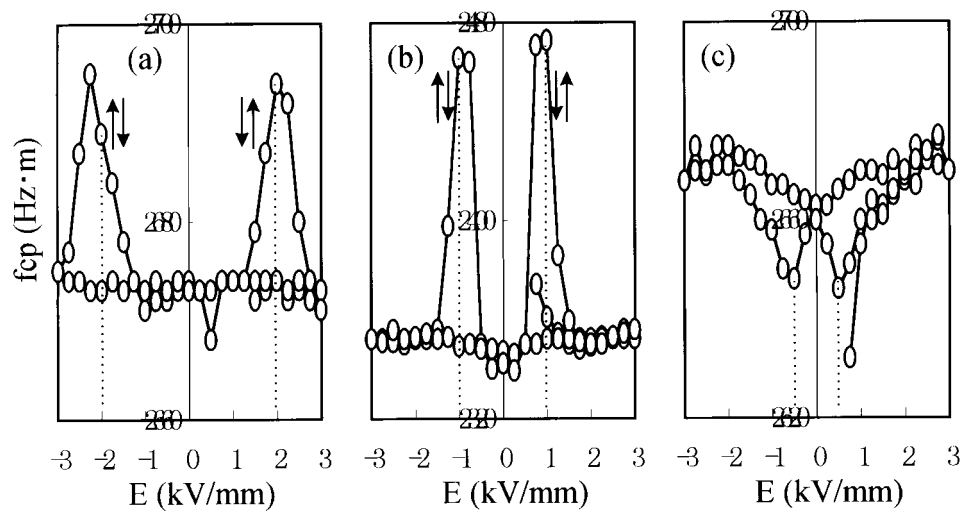


Fig. 4. Poling field ( $E$ ) dependence of frequency constant ( $f_{cp}$ ) of: (a) tetragonal, (b) M.P.B. and (c) rhombohedral PZT ceramics.

Table 1  
Domain switching and rotation by poling field

$E$ (kV/mm)	$I_{002}$	$I_{222}$	$k_p$	$\epsilon_r$	$f_{cp}$	Domain behavior by $E$
Tetragonal						
$\pm 2.0$	Min.		Min.	Min.	Max.	$180^\circ$ domain switching $+E$ $E = \pm 2.0$ $> \pm 2.0$ $90^\circ$ domain rotations $+E$ $-E$ $E < 2.0$ $> \pm 2.0$
M.P.B.						
$\pm 0.5$				Max.		
$\pm 0.75$		Min.				
$\pm 1.0$			Min.		Max.	
Rhombohedral						
$\pm 0.5$				Max.	Min.	
$\pm 0.75$		Min.				
$\pm 1.0$			Min.			
						$180^\circ$ domain switching $+E$ $E = \pm 1.0$ $> \pm 1.0$ $71^\circ, 109^\circ$ domain rotations $+E$ $-E$ $E = \pm 0.5$ $\pm 1.0$ M.P.B. Rhombohedral $E = \pm 0.5$

※  $E$  of minimum  $k_p$  corresponds to  $E_c$ .

$I(222)$ }, M.P.B. and rhombohedral) [8]. Furthermore, the dielectric and ferroelectric properties were measured using an impedance/gain-phase analyzer (HP4194A). Responses to repeated voltage pulses up to  $\pm 4.0$  kV

applied to the ceramic disks were measured at  $80^\circ\text{C}$  by a high voltage test system (Radiant: RT6000HVS). The pulse width and pulse cycle were 1 and 2  $\mu\text{s}$ , respectively.

### 3. Results and discussion

#### 3.1. Poling field dependence of $I_{002}$ and $I_{222}$

Fig. 1(a)–(c) shows the effect of  $E$  on  $I_{002}$  [(a): tetragonal] and  $I_{222}$  [(b) M.P.B. and (c) rhombohedral], respectively. Both  $I_{002}$  and  $I_{222}$  increased with increasing  $E$ . While  $I_{002}$  was almost constant except for a slight decrease at  $E = \pm 2.0$  kV/mm, a decrease in  $I_{222}$  was observed at  $\pm 0.75$  kV/mm.

#### 3.2. Poling field dependence of the planar coupling factor ( $kp$ )

The  $E$  dependence of  $kp$  is shown in Figs. 2 (a)–(c) in the case of the tetragonal (a), M.P.B. (b) and rhombohedral (c) phases, respectively. We believe the fields of the minimum  $kp$  correspond to coercive fields ( $E_c$ ). While  $E_c$  depended on the Ti/Zr ratio in the tetragonal phase, it was almost constant in the M.P.B. and rhombohedral phases. Although the  $kp$  took a minimum at

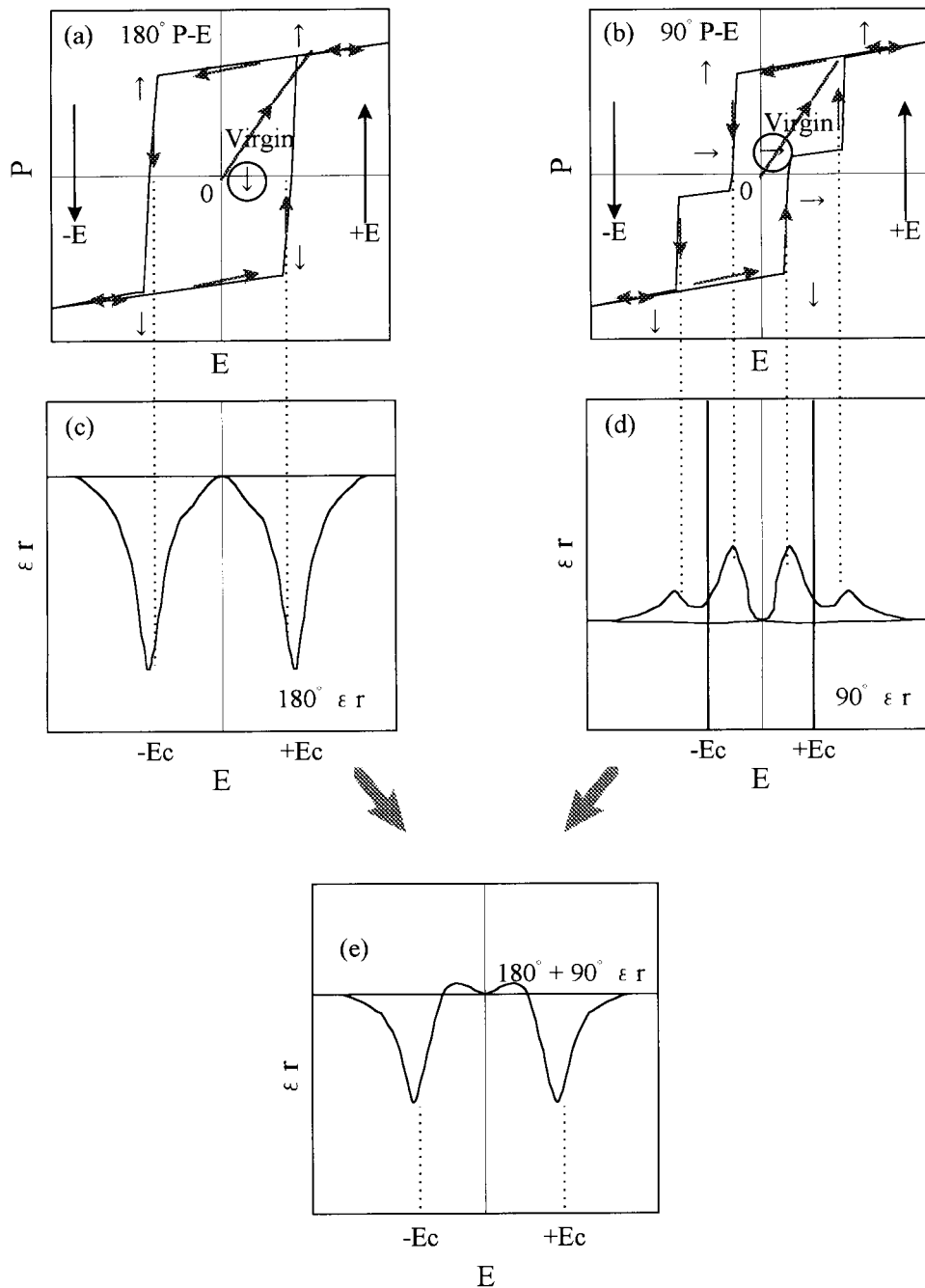


Fig. 5. Schematic P–E hysteresis loops of: (a) 180° domain switching and (b) 90° domain rotation. The effect of: (c) the switching and (d) rotation on  $\epsilon_r$ , and (e) the summation of both the  $\epsilon_r$  in case of tetragonal PZT ceramics ( $E_c = \pm 2.0$  kV/mm).

$\pm Ec$ ,  $I_{002}$  and  $I_{222}$  were almost constant under these fields in comparison with the ones of the virgin (as-fired) ceramics as shown in Figs. 1 (a)–(c). As a result, after having fully poled the virgin ceramics,  $180^\circ$  switching was the dominant factor affecting  $kp$  when alternating poling fields were applied. We believe that the minimum  $kp$  is due to the  $180^\circ$  domain switching because the electrical domain clamping [9], such as  $\uparrow\downarrow$ , occurred at the coercive fields.

### 3.3. Poling field dependence of the dielectric constant ( $\epsilon_r$ )

Fig. 3 (a)–(c) show the effect of  $E$  on  $\epsilon_r$ , when  $E$  was varied from 0 to  $\pm 3.0$  kV/mm. In the tetragonal phase,  $\epsilon_r$  took a minimum at  $\pm Ec$ . On the other hand, in M.P.B. and rhombohedral phases, after  $\epsilon_r$  decreased with increasing  $E$ , it took a maximum at  $E = \pm 0.5$  kV/mm. This confirms that  $\epsilon_r$  in the tetragonal phase decreased at  $\pm Ec$  because of the electrical domain

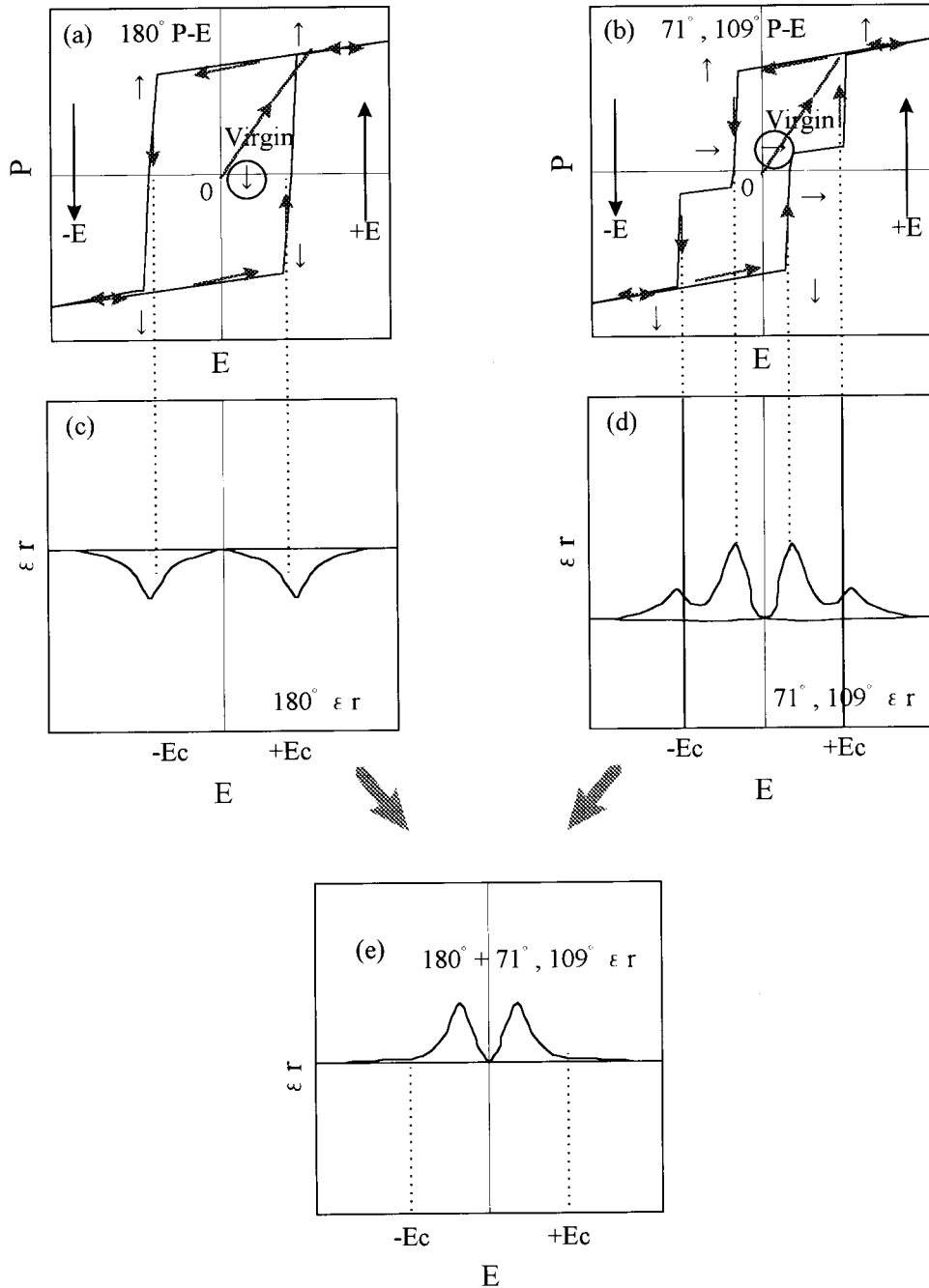


Fig. 6. Schematic P-E hysteresis loops of: (a)  $180^\circ$  domain switching and (b)  $71^\circ$  ( $109^\circ$ ) domain rotation. The effect of: (c) the switching and (d) rotation on  $\epsilon_r$ , and (e) the summation of both the  $\epsilon_r$  in case of M.P.B. and rhombohedral PZT ceramics ( $Ec = \pm 1.0$  kV/mm).

clamping. However,  $\varepsilon_r$  increased at  $E = \pm 0.5$  kV/mm in M.P.B. and rhombohedral phases because of the  $71^\circ$  and  $109^\circ$  domain rotations.

### 3.4. Poling field dependence of the frequency constant ( $f_{cp}$ )

The effect of  $E$  on  $f_{cp}$  is shown in Fig. 4 (a)–(c). While the  $f_{cp}$  in the tetragonal and M.P.B. phases took a maximum at  $\pm Ec$ , it became a minimum at  $E = \pm 0.5$  kV/mm in the rhombohedral phase, the field of which was lower than  $Ec$ . That is, when the domain clamping ( $\uparrow\downarrow$ ) occurred at  $\pm Ec$  in the tetragonal and M.P.B. phases, the  $f_{cp}$  (half the bulk wave velocity) increased because the ceramics became mechanically hard. In contrast, it took a minimum at  $E = \pm 0.5$  kV/mm in the rhombohedral phase because the ceramics became mechanically soft. We believe that the  $71^\circ$  and  $109^\circ$  domain rotations affected the  $f_{cp}$ . Furthermore, the  $E$

dependence of  $f_{cp}$  in M.P.B. showed a similar behavior as to that in the case of the tetragonal phase.

### 3.5. Domain behavior at various poling fields ( $E$ )

Table 1 shows the relationships between the maximum and minimum values of crystal orientations, the electrical properties, and the domain behavior in relation to  $E$ . When we calculated the differential of  $I_{002}$  vs.  $E$  and  $I_{222}$  vs.  $E$  ( $\Delta I_{002}/\Delta E$  and  $\Delta I_{222}/\Delta E$ ), two peaks were obtained regarding  $90^\circ$  ( $71^\circ$  or  $109^\circ$ ) rotation. Therefore, it is confirmed that  $90^\circ$  rotation occurred twice, once before and once after the  $E$  of minimum  $I_{002}$  ( $\pm 2.0$  kV/mm), in the tetragonal phase. In the M.P.B. and rhombohedral phases, the first  $71^\circ$  and  $109^\circ$  rotations occurred at  $E = \pm 0.5$  kV/mm before the  $E$  of minimum  $I_{222}$  ( $\pm 0.75$  kV/mm). The second  $71^\circ$  and  $109^\circ$  rotations occurred at  $\pm 1.0$  kV/mm after  $E = \pm 0.75$  kV/mm.

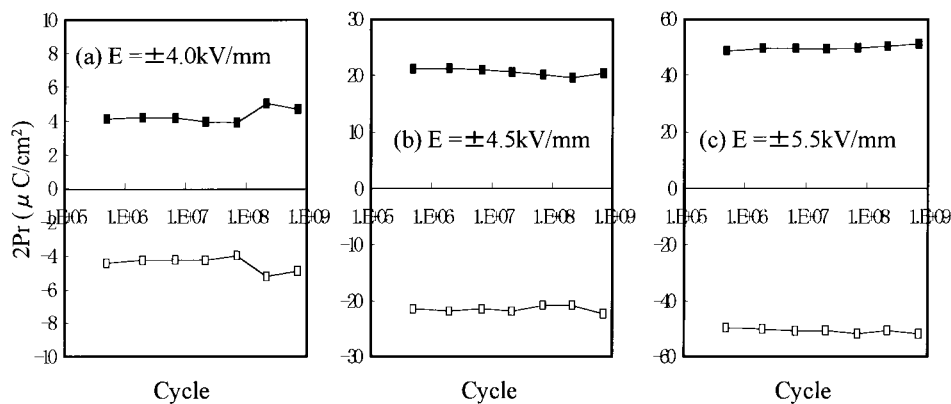


Fig. 7. Pulse cycle dependence of remanent polarization ( $Pr$ ) at: (a)  $E = \pm 4.0$  kV/mm, (b)  $E = \pm 4.5$  kV/mm and (c)  $E = 5.5$  kV/mm in the case of tetragonal PZT ceramics.

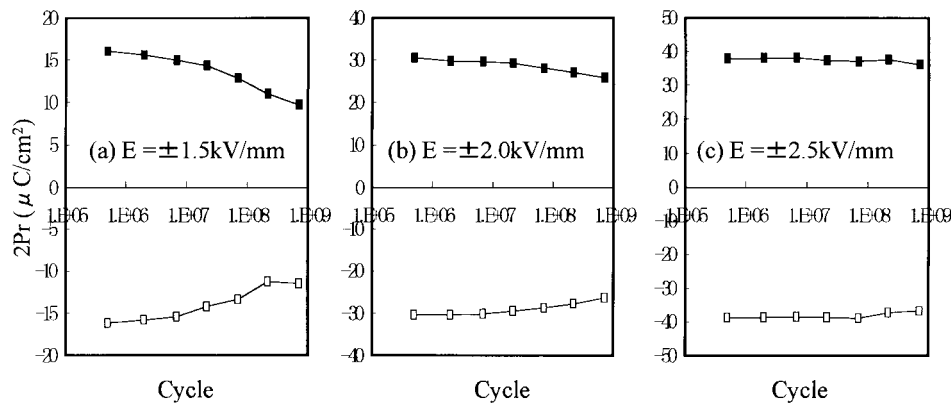


Fig. 8. Pulse cycle dependence of remanent polarization ( $Pr$ ) at: (a)  $E = \pm 1.5$  kV/mm, (b)  $E = \pm 2.0$  kV/mm and (c)  $E = \pm 2.5$  kV/mm in the case of M.P.B. PZT ceramics.

### 3.6. Effect of domain rotation and switching on dielectric constant ( $\epsilon_r$ )

The P–E hysteresis loop of 180° domain switching in tetragonal PZT ceramics as shown in Fig. 5(a) is similar to the hysteresis loop of  $kp$  vs.  $E$  [Fig. 2 (a)]. As a consequence, the poling field dependence of  $\epsilon_r$  caused by 180° switching was expected from  $dP/dE$  ( $=\epsilon_r$ ) as shown in Fig. 5(c). On the other hand, the P–E loop of 90° domain rotation shows the loop with two kinds of 90° rotation as shown in Fig. 5(b). In this case, the first rotation was caused by turning back to the initial state from a poling state and then the second rotation was due to the orientation in the direction of the poling field. Therefore, there were two peaks of  $\epsilon_r$  by rotating 90° domain as shown in Fig. 5(d), and this phenomenon corresponded to the loop of  $I_{002}$  vs.  $E$  [Fig. 1(a)]. We believe the poling field dependence of  $\epsilon_r$  could be explained by the summation of the 90° rotation and 180° switching [Figs. 5(e) and 3(a)].

Figs. 6(a)–(e) show the P–E hysteresis loops,  $dP/dE$  ( $=\epsilon_r$ ) and their summation of 180° domain switching and 71° (109°) domain rotation in M.P.B. and rhombohedral PZT ceramics, respectively. The  $E_c$  of 180°

domain P–E hysteresis loop corresponded to the  $E$  of minimum  $kp$  [ $E_c = \pm 1.0$  kV/mm in Fig. 2(b) and (c)] and the  $E_c$  of 71° (109°) domain P–E hysteresis loop was calculated from the curve of  $I_{222}$  vs.  $E$  in Fig. 1(b) and (c). Since the values of  $E$  with maximum and minimum properties were different in case of the M.P.B. and rhombohedral ceramics in comparison with the ones of the tetragonal (refer to Table 1), we could obtain the poling field dependence of  $\epsilon_r$  as shown in Figs. 6(e) and 3(b) and (c).

It was thought that the sudden decrease in  $\epsilon_r$  at  $E_c$  [Fig. 5(c)] was observed on the tetragonal ceramics in comparison with the ones of the M.P.B. and rhombohedral [Fig. 6 (c)] because of the large anisotropy ( $c/a$  ratio) of the crystal structure.

### 3.7. Pulse response measurement of transient phenomena

The pulse cycle dependence of the remanent polarization ( $Pr$ ) is shown in Figs. 7–9. The  $2Pr$  of the tetragonal, M.P.B. and rhombohedral PZT ceramics decreased with the increase of the pulse cycle at a certain voltage as shown in Figs. 7(a) and (b), 8(a) and (b), and 9(a), respectively. Further increasing the pulse voltage ( $E$ ),

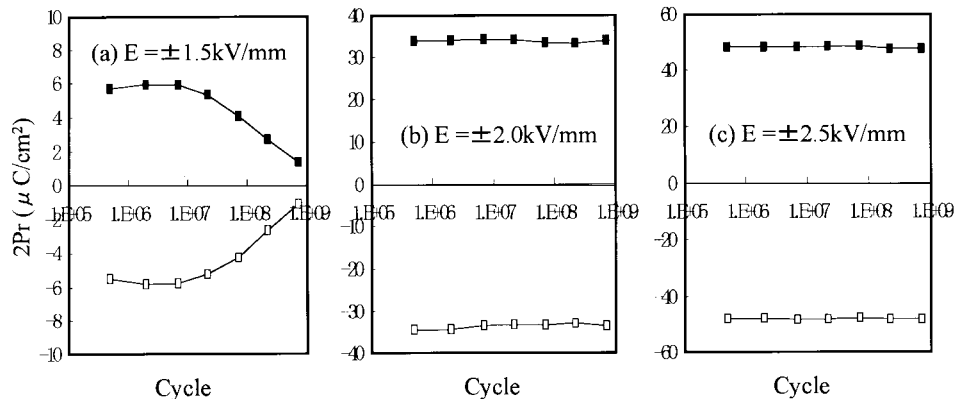


Fig. 9. Pulse cycle dependence of remanent polarization ( $Pr$ ) at: (a)  $E = \pm 1.5$  kV/mm, (b)  $E = \pm 2.0$  kV/mm and (c)  $E = \pm 2.5$  kV/mm in the case of rhombohedral PZT ceramics.

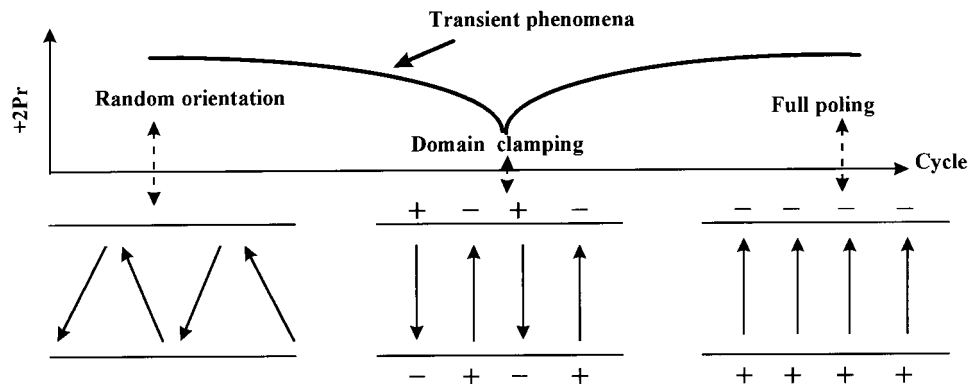


Fig. 10. Relationship between transient phenomena of remanent polarization ( $Pr$ ) and domain arrangement while applying cycle.

the polarization of  $2Pr$  was independent of the cycle as shown in Figs. 7(c), 8(c), and 9(b) and (c).

We call the decrease in polarization transient phenomena. The transient phenomena correspond to the arrangement of ferroelectric domains by applying the repeated voltage pulse. This was not “fatigue” in PZT thin films. We believe the electrical domain clamping occurred at the cycle showing the minimum polarization. Fig. 10 shows the process of domain switching in virgin (as-fired) ceramics. When  $E$  was applied to the ceramics, random orientation changes into a domain clamping state, whose value corresponded to the  $E_c$  as the static evaluation. After that, further increasing  $E$ , this state changed into orientation polarization. The pulse response measurement became an effective tool to dynamically analyze the ferroelectric domain switching in PZT ceramics.

#### 4. Conclusions

The domain structures in PZT ceramics were statically evaluated at various poling fields to investigate the poling field dependence of the crystal orientations and electrical properties. Moreover, the domain structures were dynamically evaluated by the pulse response measurement.

Our investigations clarified the effect of the domain structures on the electrical properties.

#### Acknowledgements

This work was partly supported by a Grant-in-Aid for Scientific Research (C) (No. 09650370) from the Japanese Ministry of Education, Science and Culture, and the Tong Yang Central Laboratories in Korea.

#### References

- [1] A. Yamada, Y.K. Chung, M. Takahashi, T. Ogawa, *Jpn. J. Appl. Phys.* 35 (1996) 5232.
- [2] A. Yamada, T. Ogawa, M. Takahashi, Y.K. Chung, *Trans. Mater. Res. Soc. Japan* 20 (1996) 603.
- [3] T. Ogawa, Y. Takeshita, T. Miyamoto, D.I. Chun, *Ferroelectrics* 186 (1996) 119.
- [4] T. Ogawa, *Ferroelectrics* 169 (1995) 55.
- [5] C.C. Li, X.W. Zhang, Y.J. Xia, *Ferroelectrics* 37 (1981) 623.
- [6] K. Mehta, A.V. Virkar, *J. Am. Ceram. Soc.* 73 (1990) 567.
- [7] T. Ogawa, *Ceram. Bull.* 70 (1991) 1042.
- [8] T. Ogawa, A. Yamada, *Proceedings of the 8th US–Japan Seminar on Dielectric and Piezoelectric Ceramics*, 1997, p. 268.
- [9] T. Ogawa, A. Yamada, Y.K. Chung, D.I. Chun, *Korean Phys. Soc.* 32 (1998) S724.